



# Local structure and magnetic properties of ferromagnetic GaMnAs made by helium ion induced epitaxial crystallization annealing



C.H. Chen<sup>a,b,\*</sup>, H. Niu<sup>b</sup>, D.C. Yan<sup>c</sup>, H.H. Hsieh<sup>d</sup>, R.T. Huang<sup>e</sup>, C.C. Chi<sup>f</sup>, C.P. Lee<sup>a</sup>

<sup>a</sup> Center for Nano Science and Technology, National Chiao Tung University, HsinChu 30010, Taiwan

<sup>b</sup> Nuclear Science and Technology Development Center, National Tsing Hua University, HsinChu 30013, Taiwan

<sup>c</sup> Green Energy and Environment Research Laboratories, Industrial Technology Research Institute, ChuTung, HsinChu 31040, Taiwan

<sup>d</sup> Department of Electrical Engineering, Chung Cheng Institute of Technology, National Defense University, 33551, Taiwan

<sup>e</sup> Institute of Materials Engineering, National Taiwan Ocean University, Keelung 20224, Taiwan

<sup>f</sup> Department of Physics, National Tsing Hua University, HsinChu 30013, Taiwan

## ARTICLE INFO

### Article history:

Received 30 November 2013

Received in revised form 22 March 2014

Accepted 22 March 2014

Available online 31 March 2014

### Keywords:

Diluted magnetic semiconductor

Ferromagnetism

Ion implantation

Ion beam induced epitaxial crystallization

## ABSTRACT

In this study we show GaMnAs preparation by Mn implantation in GaAs followed by helium ion beam induced epitaxial crystallization annealing. The characteristics of the Mn-implanted layer were investigated by X-ray diffraction, and transmission electron microscopy. The magnetic nature of the Mn-implanted layer was investigated with a superconducting quantum interference device. Structure analysis showed that Mn ions were incorporated substitutionally into the GaAs lattice without the formation of any detectable secondary phases. The remanent magnetic moment exhibited room temperature ferromagnetism. Additional measurement using X-ray magnetic circular dichroism also revealed that the carriers were spin polarized.

© 2014 Elsevier B.V. All rights reserved.

## 1. Introduction

Diluted magnetic semiconductors (DMSs) have attracted considerable attention because of their potential applications in spintronics [1–3]. GaMnAs, a group of III–V DMSs [4,5], have received considerable attention in recent years because of agreement of experimental data with theoretical model. Ion beam induced epitaxial crystallization (IBIEC) [6–8] is known as an approach to recrystallize thin films at low temperature and in ultra-short time. In this study, we have attempted to prepare ferromagnetic GaMnAs thin films using this methods [9,10]. In our previous study, ion channeling results on GaMnAs showed that most implanted Mn ions are located at substitutional sites and the implanted layer was re-crystallized well after IBIEC [10]. In this work, we report characteristics of IBIEC treated Mn implanted GaAs investigated by double crystal X-ray diffraction (DCXRD), transmission electron microscopy (TEM) and superconducting quantum interference device (SQUID).

## 2. Experiment and method

GaMnAs films were fabricated using single crystal SI-type (001) GaAs wafers. These were multi-implanted by Mn<sup>+</sup> ions with energies 70, 120, 170, 250, and 350 keV to an average dose for a uniformly distribution at room temperature. The corresponding atomic concentrations were controlled by Mn<sup>+</sup> implantation dose between 5.5E14 and 2.2E16 cm<sup>-2</sup>, corresponding to 0.25–10 at.% of Mn. The samples' substrate temperature was kept at room temperature during Mn implantation. Post annealing was done by IBIEC treatment using 0.4 μA cm<sup>-2</sup> 350 keV He ion beam irradiating samples for 2 h with substrate temperature kept at 523 K. The newly Mn-implanted GaAs wafers were etched in modified Standard Clean-1 solution to remove the surface oxide; then they were cleaned in ethanol and acetone for two minutes each with ultrasonic tank. The cleaning procedure was also performed after ion implantation and IBIEC to prevent other possible magnetic sources from being absorbed on the sample surface. The X-ray absorption spectrum (XAS) and X-ray magnetic circular dichroism (XMCD) measurements were carried out at Mn L edge on the 11 beamline at National Synchrotron Radiation Research Center. Magnetic properties were measured using Quantum Design MPMS-2.

\* Corresponding author at: Center for Nano Science and Technology, National Chiao Tung University, HsinChu 30010, Taiwan. Tel.: +88635742886.

E-mail address: [akiracc@gmail.com](mailto:akiracc@gmail.com) (C.H. Chen).

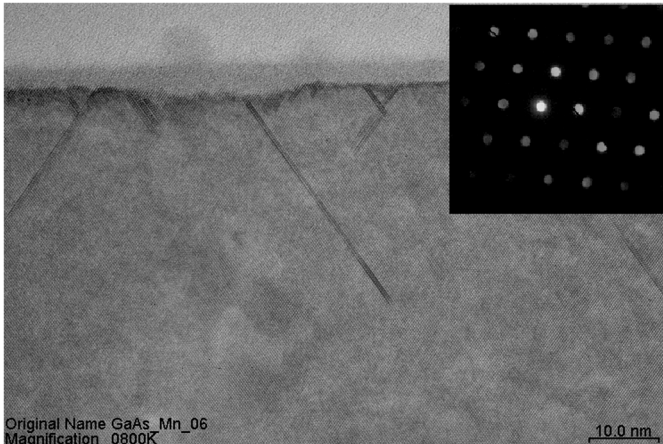


**Fig. 1.** TEM images of IBIEC-annealed GaMnAs sample. The inset is the SAD pattern which is selected from the regrowth area.

### 3. Results and discussion

In order to correlate structure and magnetic properties, we investigated recrystallization after IBIEC annealing by means of HRTEM, DCXRD and SQUID measurement.

Fig. 1 shows the high-resolution transmission electron microscopy (HRTEM) images of an IBIEC-annealed GaMnAs sample. The HRTEM was carried out on the 2.6 at.% sample and provided mainly its crystalline structure. The figure shows that the implanted region of the IBIEC-annealed GaMnAs sample was almost regrowth after IBIEC treatment. The clear diffraction points of selected-area electron diffraction pattern (SAD) indicate good crystallinity. The lattice image shown in Fig. 1 also indicates that the crystal has been repaired. And in the lattice image, one cannot find any evidence of heterostructure of a secondary phase (either GaMn alloys or MnAs clusters) in the image. In addition, we also performed energy-dispersive X-ray spectroscopy (EDX) to determine Mn concentration in the layer. The area selected for EDX measurement was about 10 nm in radius. The Mn concentrations of the Mn-implanted layer measured by EDX were around 0.7–1.0%. We found no significant large Mn concentration in the region. Even in the dislocation region, Mn concentration was around 0.8%.

HRTEM and EDX measurements do not show any hints of GaMn alloys or MnAs clusters formation. Therefore, the next step in our experiment on DCXRD was carried out on the 3.5 at.% sample and it provided mainly similar information about lattice constant, strain, relaxation, and crystalline perfection related to the composition. In Fig. 2 the  $\omega$ - $2\theta$  scans of the Mn 3.5 at.% samples are presented. The wavelength of the X-ray was  $\text{CuK}_{\alpha 1}$  (0.1542 nm) which was selected by double Si (1 1 1) single crystals. The XRD spectra of the GaMnAs thin film around the GaAs (0 0 4) peak before and after IBIEC annealing are displayed. After the IBIEC annealing, however, an additional shoulder peak appeared on the smaller angle side of the GaAs (0 0 4) peak. This indicates the formation of a compressively strained GaMnAs film [1]. We also checked GaAs (2 2 4) and GaAs (3 1 1) peaks, and similar shoulder peaks were observed. In order to make sure there was no second phase formation, we carefully scanned the XRD spectrum without CCC mode, even in the logarithmic scale, using grazing incidence X-ray diffraction. All the IBIEC annealed GaMnAs samples showed highly crystallized structure without the formation of secondary phases [11,12].

It was found that the lattice constant for the content of Mn did not met with the prediction by Vegard's law [1]. According to Vegard's law, the concentration of Mn is proportional to the lattice constant. But the results of DCXRD measurement found it did not

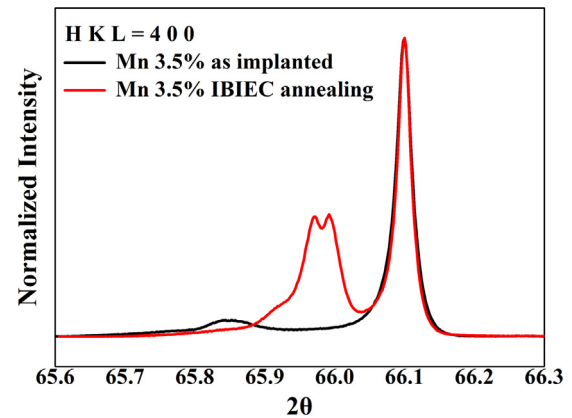


**Fig. 2.** DCXRD  $\omega$ - $2\theta$  scan revealing the formation of GaMnAs, at the low angle side of the Ge (0 0 4) peak after IBIEC annealing.

agree with this law for all samples. It might indicate the existence of strain in the GaMnAs layer.

The XMCD experiment was performed to study the electronic structure of doped Mn ions and the sample's origin of ferromagnetism. The L-edge X-ray absorption spectrum (2p-XAS) and XMCD signals of the samples were measured either with total electron yield (TEY) or total fluorescence yield (TFY). Here the energy resolution of synchrotron radiation was set to 0.4 eV. Fig. 3 shows the TEY of XMCD for the 2p-3d transitions of Mn. The measurement was carried out at 77 K for the sample with 4% Mn. The difference of the XAS spectra at  $2p_{1/2}$  and  $2p_{2/3}$  obtained by excitations from opposite circularly polarized light indicates that the origin of ferromagnetism is indeed from the unpaired d shell electrons of Mn atoms. The characteristics of the 2p-XAS spectrum were also used to assess the electronic valence state of Mn ions in the GaAs matrix. From the  $2p_{3/2}$  peak positions in TEY and the sharp peaks of TEY we may infer that the electronic valence state was  $2^+$  [13,14]. The  $2^+$  valence state also indicates that Mn ions are on the Ga substitutional sites in the GaAs lattice. The above results also provide evidence that the Mn ions serve as acceptors in GaAs and the hole carriers are spin polarized to carry the magnetic property of the material [15].

The samples, from which the structure was analyzed were also studied by SQUID magnetometry. All the samples were cut into ca. 2 mm × 2 mm–3 mm × 3 mm for fitting the diameter of the plastic straw used on the SQUID. Fig. 4 shows the remanent moments of the samples with 2% content of Mn and also different contents of Mg. The remanent moments were measured after 1 T field-cooled

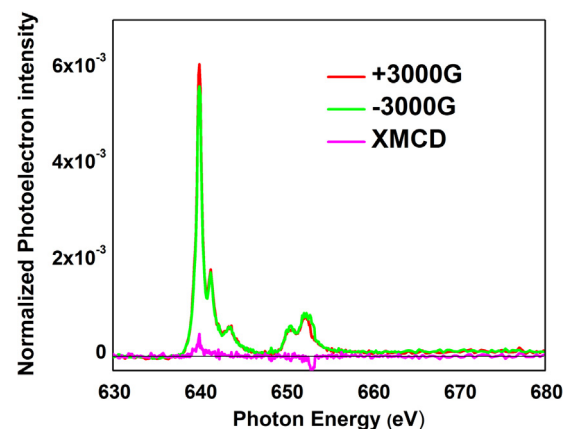


**Fig. 3.** Experimental Mn 2p-XAS spectra of the GaMnAs measured by TEY at 77 K. The MCD signal is obtained from the difference in the spectra.

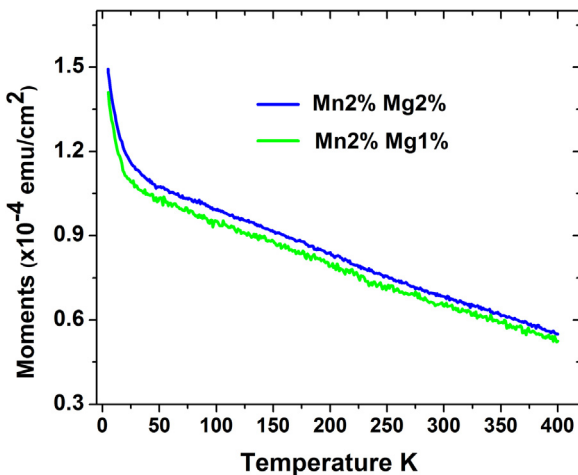


**Fig. 4.** The remanent magnetization, measured with a 1 T field cooled process. Temperature dependence of the remanent magnetizations for samples with 2% Mn concentration and different co-doped Mg concentration. It shows the higher co-doped Mg sample exhibit higher magnetization.

process from 400 K to 5 K. The remanent moments of both samples show the GaMnAs layers retain their ferromagnetism even above 400 K. Fig. 4 also shows that the temperature dependence of remanent moments are increasing with doped Mg concentration. Fig. 5 shows the remanent magnetic moments of the sample with 2% content of Mn and 2% contents of Mg. The measured remanence shows the significant anisotropy in both of (0 0 1) and (0 1 1) directions. Fig. 6 shows field dependent magnetization in both (0 1 1) and (0 0 1) axes at 5 K. The sample shows strong anisotropy in the (0 1 1) axis [1]. In the (0 1 1) axis, it shows a clear hysteresis loop. The sample was saturated at 600 G. As shown in Fig. 6, the measured saturated moment is about  $2.92 \times 10^{-4}$  emu/cm<sup>2</sup> at 5 K. According to the implanted Mn dose of this sample, its theoretical magnetic moment  $M$  is  $3.47 \times 10^{-4}$  emu/cm<sup>2</sup>, where  $M = gN_{\text{Mn}}\mu_{\text{b}}$  [1],  $g$  is the Landé  $g$ -factor,  $N_{\text{Mn}}$  is area density of implanted Mn and  $\mu_{\text{b}}$  is the Bohr magneton. Using this formula to estimate the effective magnetic moment is about  $2.1 \mu_{\text{b}}$  (84%).

The results of SQUID measurements indicate that all GaMnAs samples had ferromagnetism even above room temperature. It is usually considered that room temperature ferromagnetism has

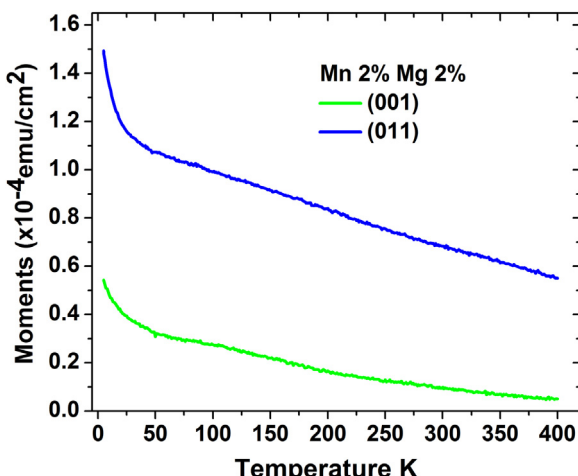


**Fig. 5.** The remanent magnetization was measure with a 1 T field cooled process. Temperature dependence of the remanent magnetizations for samples with 2% Mn concentration and 2% Mg concentration. The remanent magnetization was measured in both (0 0 1) and (0 1 1) directions along with applied magnetic field. It shows clear the easy axis is lied on the (0 1 1) axis.

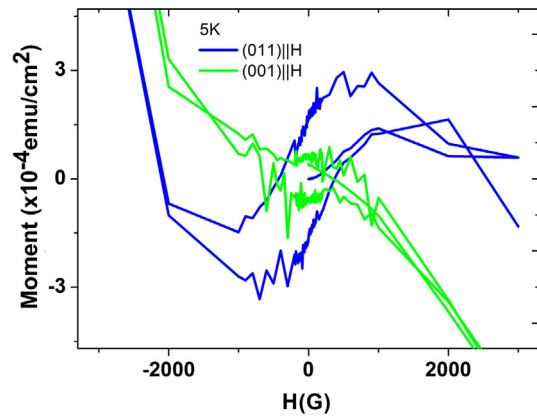


**Fig. 6.** Field dependent magnetization for a 2.6% Mn sample at 5 K. The magnetization (expressed in number of Bohr magneton per Mn ion) was obtained by dividing the measured magnetization by the total dose of the implanted Mn atoms. The saturated moment is  $2.1 \mu_{\text{b}}$  ( $2.92 \times 10^{-4}$  emu/cm<sup>2</sup>) at 5 K and magnetization reached saturation around 0.06 T.

come from a secondary phase in the GaMnAs layer, but here the possibility of the secondary phase formation in the GaMnAs layers was excluded by the structure analysis and our previous channeling study [9]. Then, there are two possibilities for the origin of the ferromagnetism. One is that the ferromagnetism comes from the GaMnAs alloy, the other is that the ferromagnetism comes from a secondary phase that is not detectable with the analysis tools that we used. The substitutional rate of Mn of GaMnAs estimated previously by PIXE/w channeling is up to 74% [9]. And in the Mn 2.6% sample, up to 84% of Mn ions participate in the ferromagnetism which was determined by SQUID. So the ferromagnetism should come from GaMnAs alloy, and its monotonically decreasing moment behavior is similar to that of a coherent Mn enriched GaMnAs sample which was prepared at low temperature-MBE [16].

To summarize: The structural properties of GaMnAs have been presented. The HRTEM results indicate a recrystallized, ca. 300 nm thick GaMnAs top layer. The DCXRD results show a strained layer after implantation. The IBIEC annealed GaMnAs displays one additional peak for lower angle which represents the larger lattice parameter of GaMnAs and the lattice of GaMnAs is coherent with the lattice of GaAs substrate. It does agree with our previous ion channeling structure analysis and HRTEM result.

The formation of the compressively strained GaMnAs film was also confirmed by a separate study using magnetic hysteresis measurement. Because the easy axis lies in the [1 1 0] direction [1]. For the previous ion channeling studies for GaMnAs samples, we found that the crystals were almost repaired. An angular scan of ion channeling found that the strain varied with depth from the surface to the end of the GaMnAs layer. It suggests compressive strain formed in the GaMnAs layer and the magnitude of the strain varied with depth in the GaMnAs layer. If the GaMnAs layer is fully relaxed from the GaAs substrate, the results of XRD should be consistent with Vegard's law. So it is reasonable to deduce the existence of strain in the GaMnAs/GaAs layer.

#### 4. Conclusion

In this work, we had performed HRTEM and DCXRD studies on GaMnAs thin films made by ion implantation and followed by IBIEC annealing. We could find no evidence of an observable secondary phase in the GaMnAs layer. The magnetic measurements show room temperature ferromagnetism. From XAS and XMCD measurements, it was concluded that the valence state of Mn is 2+, and the carriers in the GaMnAs thin film are spin polarized. This

implies that the origin of ferromagnetism of the thin film is not from a secondary phase.

## Acknowledgment

This work was supported by the National Science Council (Grant No. NSC102-2221-E-009-045).

## References

- [1] H. Ohno, A. Shen, F. Matsukura, A. Oiwa, A. Endo, S. Katsumoto, Y. Iye, *Appl. Phys. Lett.* 69 (1996) 363–365.
- [2] H. Munekata, H. Ohno, S. von Molnar, A. Segmüller, L.L. Chang, L. Esaki, *Phys. Rev. Lett.* 63 (1989) 1849.
- [3] H. Ohno, *Science* 281 (1998) 951–956.
- [4] F. Matsukura, A. Oiwa, A. Shen, Y. Sugawara, N. Akiba, T. Kuroiwa, H. Ohno, A. Endo, S. Katsumoto, Y. Iye, *Appl. Surf. Sci.* 113–114 (1997) 178–182.
- [5] D. Chiba, A. Werpachowska, M. Endo, Y. Nishitani, F. Matsukura, T. Dietl, H. Ohno, *Phys. Rev. Lett.* 104 (2010) 106601.
- [6] N. Kobayashi, M. Hasegawa, N. Hayashi, *Nucl. Instrum. Methods Phys. Res. B: Beam Interact. Mater. Atoms* 80–81 (1993) 790–794.
- [7] R. Schulz, T. Bachmann, U. Kaiser, E. Glaser, *Nucl. Instrum. Methods Phys. Res. B: Beam Interact. Mater. Atoms* 117 (1996) 207–209.
- [8] J. Linnros, B. Svensson, G. Holmén, *Phys. Rev. B* 30 (1984) 3629–3638.
- [9] C.H. Chen, H. Niu, C.Y. Cheng, H.H. Hsieh, Y.C. Yu, S.C. Wu, *Nucl. Instrum. Methods Phys. Res. B: Beam Interact. Mater. Atoms* 261 (2007) 570–573.
- [10] C.H. Chen, H. Niu, C.Y. Cheng, H.H. Hsieh, S.C. Wu, *Nucl. Instrum. Methods Phys. Res. B: Beam Interact. Mater. Atoms* 266 (2008) 1734–1736.
- [11] S.-L. Song, N.-F. Chen, J.-P. Zhou, Z.-G. Yin, Y.-L. Li, S.-Y. Yang, Z.-K. Liu, *J. Cryst. Growth* 264 (2004) 31–35.
- [12] J. Yang, N. Chen, Z. Liu, S. Yang, C. Chai, M. Liao, H. He, *J. Cryst. Growth* 234 (2002) 359–363.
- [13] J. Okabayashi, M. Oshima, *NSRRC Activity Report*, 2002/2003, pp. 48–51.
- [14] P. Gambardella, L. Claude, S. Rusponi, K.J. Franke, H. Brune, J. Raabe, F. Nolting, P. Bencok, A.T. Hanbicki, B.T. Jonker, C. Grazioli, M. Veronese, C. Carbone, *Phys. Rev. B* 75 (2007) 125211.
- [15] S. Ahlers, P.R. Stone, N. Sircar, E. Arenholz, O.D. Dubon, D. Bougeard, *Appl. Phys. Lett.* 95 (2009) 151911.
- [16] M. Yokoyama, H. Yamaguchi, T. Ogawa, M. Tanaka, *J. Appl. Phys.* 97 (2005) 10D317.